Biophysical Journal, Volume *122*

Supplemental information

Brownian dynamics simulations of mesoscale chromatin fibers

Zilong Li, Stephanie Portillo-Ledesma, and Tamar Schlick

Brownian Dynamics Simulations of Mesoscale Chromatin Fibers Supporting Information

Zilong Li[1], Stephanie Portillo-Ledesma[1], and Tamar Schlick[1,2,3]

[1]Department of Chemistry, 100 Washington Square East, Silver Building, New York University, New York, NY 10003 U.S.A.
[2]Courant Institute of Mathematical Sciences, New York University, 251 Mercer St., New York, NY 10012 U.S.A.
[3]New York University-East China Normal University Center for Computational Chemistry, New York University Shanghai, Shanghai 200122 China.

May 2022

1 Overview on overall strategy, difficulties, and approach

1.1 Strategy

To efficiently perform Brownian Dynamics (BD) simulations, we combine these key elements: our chromatin mesoscale model, our chromatin BD algorithm developed earlier [1], and the CUDA (Compute Unified Device Architecture) platform to run simulations on GPUs.

- Our mesoscale model for chromatin has evolved for 20 years [2, 3] to accurately reproduce experimental results on chromatin folding. It contains coarse grained units for the nucleosome cores [4], irregular linker DNA [5], histone tails [6], and linker histone (LH) [7]. Besides, it can treat histone tail acetylation [8, 9] and several LH binding modes and variants [10]. This makes it an excellent model to study chromatin at the nucleosome level.
- Our BD algorithm for chromatin was developed by Beard and Schlick [1] with Rotne-Prager hydrodynamic tensor using the second-order integration.
- We develop the code with the CUDA application for computing on GPUs, significantly speeding up calculations by massive parallelization.

1.2 Difficulties

The main difficulties encountered during the development were associated to the calculation of the hydrodynamic interactions, presence of non-calculation latencies associated to GPU computing, scientific correctness, and sampling issue.

- In the BD algorithm, we have a very large hydrodynamic interactions (HI) matrix that consumes memory with space complexity $O(n^2)$ and computational time associated with its Cholesky factorization with a time complexity of $O(n^3)$ for n particles.
- In the CUDA code, there are non-calculation latencies coming from using threads belonging to different blocks in the GPU. This increases data sharing time, consuming most of the wall time.
- The Brownian Dynamics strategy has been proposed over 40 years [11] and applied on many models but mostly coarse grained models. Our mesoscale model was used in MC simulations, but some artificial parameters cannot be used directly in BD (i.e., excluded volume).
- Similar to other simulation techniques, we faced the equilibrium sampling problem. As the system size increases, the time to fold fibers increases considerably.

1.3 Approach

- We assign many threads to calculate the large HI and force matrices and let each thread handle one calculation, converting the complexity from $O(n^2)$ to $O(1)$. For the Cholesky decomposition, we use the well-developed library "cuSolver" that calculates the matrix column by column in parallel and reduces the complexity from $O(n^3)$ to $O(n)$.
- To reduce non-calculation latencies as much as possible, we reduce the data transfer between GPU and CPU by completing most of the calculations in GPU, even those that were not computing intensive in CPU.
- To improve the scientific correctness we run at least 5 independent replicas for every simulation and compared with different experimental data with different perspectives and setups. Many sets of parameters were tested and justified according to the comparison of the experimental data when developing the BD code.
- The current solution for the sampling problem is to use Monte Carlo simulations to obtain equilibrated and folded fibers and then use BD to study their dynamics.

2 Chromatin Mesoscale Model

2.1 Components and their Connection

The coarse-grained chromatin model consists of nucleosome cores [4], treated as disks; and linker DNA [12], histone tails [13], and LHs [7, 10], treated as beads (Figure 1).

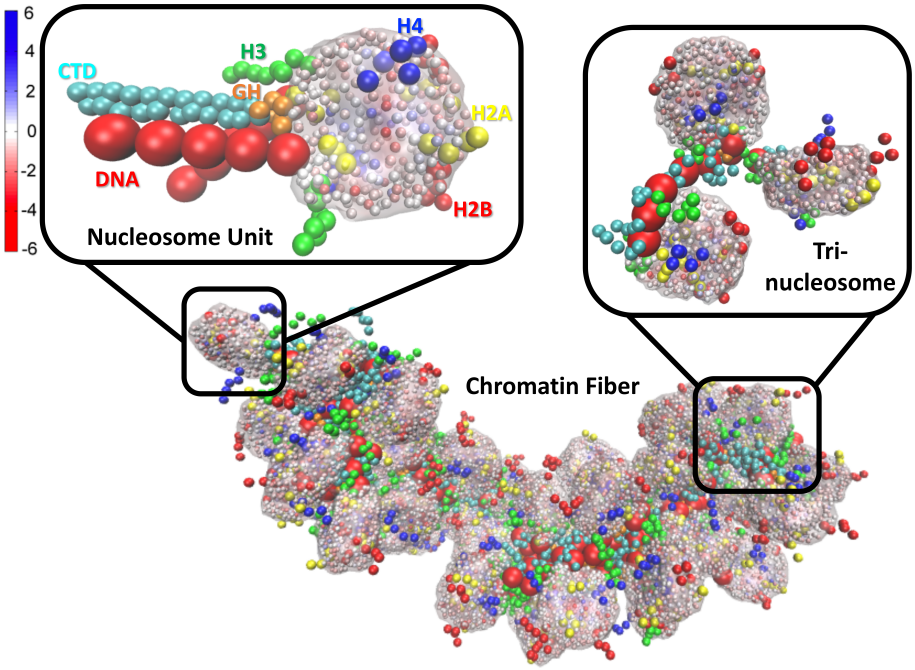

Figure 1: Chromatin mesoscale model. 50-nucleosome chromatin fiber with enlarged basic unit (chromatosome) showing each element, and enlarged tri-nucleosome showing the connection between nucleosomes by linker DNA. Linker DNA is shown as red beads, histone tails as green (H3), yellow (H2A), red (H2B), and blue (H4) beads, LHs are shown as orange (globular head) and cyan (C-terminal domain) beads, and nucleosome cores are shown with their distributed charge beads.

Our collective chromatin model can be regarded as springs connecting balls. In particular, linker DNAs connect nucleosome cores, and histone tails and LHs are attached to the nucleosome cores. Each bead can move freely during the simulation, except for the 300 charge beads in the nucleosome cores, one fixed tail bead per histone tail, and the 6 LH globular head (GH) beads, which must move together with the nucleosome core. Hence, the coarse-grained chromatin model has flexible linker DNA, histone tails and LHs, and rigid nucleosome cores.

Linker DNA – Nucleosome Core Connection The nucleosome core with 1.7 turns of DNA wrapped around is modeled as a disk [14]. Each linker DNA bead connecting nucleosomes represents roughly 9 base-pairs (detailed conversion in Equation 16). To simulate the wrapped DNA supercoil as observed experimentally, the linker DNA is not connected to the center, but to the imaginary points on the nucleosome core disk, as shown in Figure 2. Each nucleosome core disk has a radius of $r_0 = 4.8\ nm$, and parameters $w_0 = 1.8\ nm$, $\theta_0 = 108^o$ determined by the geometry of the wrapped DNA supercoil. We assign an Euler body-centered coordinate frame to each linker DNA bead and each core disk. For the Euler frame $\{\boldsymbol{a_i}, \boldsymbol{b_i}, \boldsymbol{c_i}\}$ of the core disks, the unit vectors $\boldsymbol{a_i}$ and $\boldsymbol{b_i}$ are parallel to the plane of the flat surface of the disk, while $\boldsymbol{c_i}$ is perpendicular to it. Thus, the location of the two imaginary points can be represented by:

$$\mathbf{r}_i^- = \mathbf{r}_i - r_0(-sin(\theta_0)\mathbf{a}_i + cos(\theta_0)\mathbf{b}_i) + w_0\mathbf{c}_i, \tag{1}$$

$$\mathbf{r}_i^+ = \mathbf{r}_i - (r_0\mathbf{b}_i + w_0\mathbf{c}_i). \tag{2}$$

The Euler frames on the linker DNA are updated during each step of the simulation so that the unit vector $\boldsymbol{a_i}$ is always pointing to the next bead (to the imaginary point on the nucleosome core disk if the next "bead" is a nucleosome core disk).

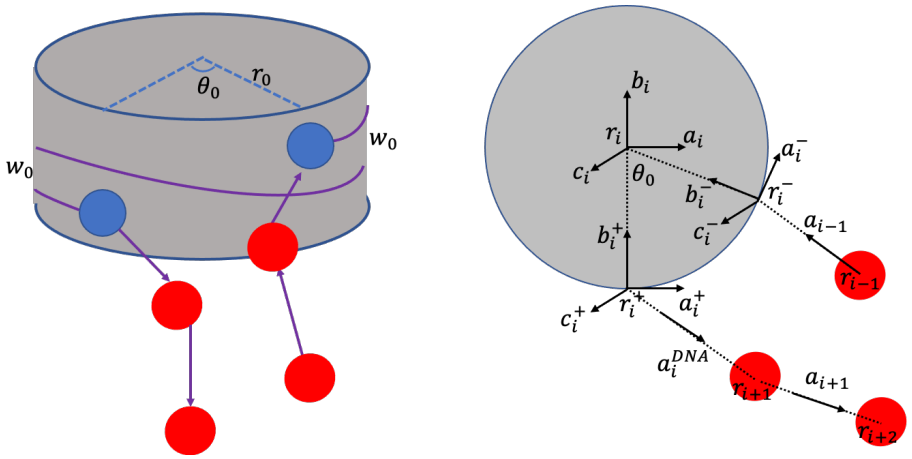

Figure 2: Relative positions of linker DNA and nucleosome core. Red beads represent linker DNA, the grey disk is the nucleosome core, and blue beads are imaginary points embedded on the nucleosome core to connect linker DNA. At left, we show the DNA supercoil and linker DNA entering and leaving the nucleosome. At right, we show the assigned Euler vectors.

Histone Tails – Nucleosome Core Connection The histone tail geometry and parameters are adopted from our previous work in [13], as shown in Figure 1. Each nucleosome core disk has 10 histone tails: two N-terminal domains of H2A (yellow beads), H2B (red beads), H3 (green beads), and H4 (blue beads), and two C-terminal domains of H2A (yellow beads). Each tail is treated as a spring with one bead fixed on the nucleosome core.

Linker Histone – Nucleosome Core Connection The LH geometry and parameters are adopted from our earlier works in [7, 10]. The coarse-grained model contains 6 beads for the GH and 22 beads for the C-terminal domain, as shown in Figure 1.

2.2 Euler Angle

Since we have defined Euler frames on the linker DNA and nucleosome cores, Euler Angles describing the relative position between beads are also calculated, and are used to calculate bending and twisting energies and force terms discussed in the following sections.

As discussed in Section 2.1, the Euler frames are updated during each step of the simulation so that the unit vector $\boldsymbol{a_i}$ always pointing to the next bead. Thus, β, shown in Figure 3, is calculated as:

$$\beta_i = \arccos(\mathbf{a}_i \cdot \mathbf{a}_{i+1}). \tag{3}$$

The other two Euler angles, α and γ, also shown in Figure 3, are defined as follows: $\boldsymbol{p}$ is the vector perpendicular to $\boldsymbol{a_i}$ and $\boldsymbol{a_{i+1}}$, α is the angle between $\boldsymbol{b_i}$ and $\boldsymbol{p}$, and γ is the angle between $\boldsymbol{p}$ and $\boldsymbol{b_{i+1}}$:

$$\alpha_i = \arccos\left(\frac{\mathbf{a}_{i+1}\cdot\mathbf{b}_i}{\sin(\beta_i)}\right), \tag{4}$$

$$\gamma_i = \arccos\left(\frac{\mathbf{b}_i\cdot\mathbf{b}_{i+1}+\mathbf{c}_i\cdot\mathbf{c}_{i+1}}{1+\cos(\beta_i)}\right) - \alpha_i. \tag{5}$$

For the nucleosome core, the linker DNA is connected to the two imaginary points on the disk. Thus, the Euler frames assigned on these two points are used instead of these assigned to the center of the core. An additional set of Euler angles $\{\alpha_i^+, \beta_i^+, \gamma_i^+\}$ is also calculated representing the Euler transformation from $\{\boldsymbol{a}_i^+, \boldsymbol{b}_i^+, \boldsymbol{c}_i^+\}$ to $\{\boldsymbol{a}_i^{DNA}, \boldsymbol{b}_i^{DNA}, \boldsymbol{c}_i^{DNA}\}$, as shown in Figure 2.

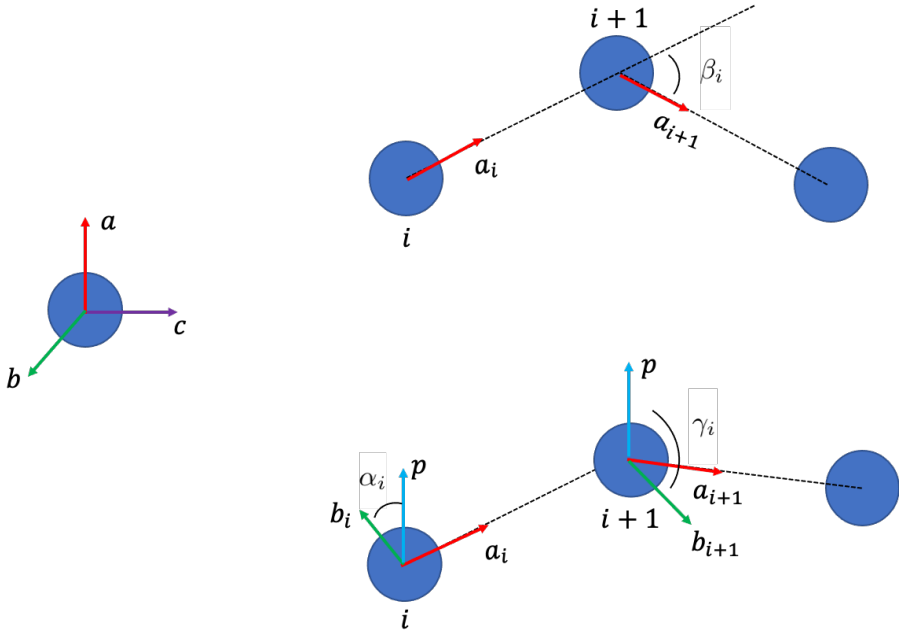

Figure 3: Schematic representation of Euler Angle related with Euler frames.

3 Energy

There are 5 types of energy terms calculated during a BD simulation that make up the effective force. These are stretching, bending, twisting, electrostatic, and excluded volume energies. The details of each energy term and the beads they applied to are given below.

3.1 Stretching

The stretching energy between two beads is based on Hooke's law, and given by:

$$E_{S_i} = \frac{h}{2}(l_i - l_0)^2, \tag{6}$$

where h is the stretching constant, l_i is the distance between two beads, and l_0 is the equilibrium length.

The stretching energy is calculated for linker DNA and nucleosome core, histone tails, LHs, and histone tails and nucleosome core.

Linker DNA – Nucleosome Core The stretching energy between linker DNA and nucleosome cores, more specifically between a DNA bead and a reference point on the nucleosome core disk (Figure 2), is the summation of stretching energy between each two adjacent beads.

$$E_S = \frac{h}{2}\sum_{i=1}^{N-1}(l_i - l_0)^2, \tag{7}$$

where $h = \frac{100k_BT}{{l_0}^2}$, with k_B the Boltzmann's constant, T the temperature, and $l_0 = 3\ nm$.

Histone tails For the histone tails, each tail is treated as a spring, so the stretching energy is the summation of all the stretching energies calculated by each tail on all the nucleosome cores as follows:

$$E_{tS} = \sum_{i=1}^{N_c}\sum_{j=1}^{N_t}\sum_{k=1}^{N_j-1}\frac{k_{jk}}{2}(l_{ijk} - l_{jk0})^2, \tag{8}$$

where, N_c is the number of cores, N_t the number of tails per core, and N_j the number of beads per tail (each tail has different number of beads, as shown in Figure 1). The parameters k_{jk} and l_{jk0} are taken from our previous work in [13], and are shown in Table 1.

Table 1: Histone tail parameters for the stretching energy term

Tail	Bond j-k	k_{jk} $(kcal/mol/\text{Å})$	l_{jk0} [Å]
N-ter H3	1-2	0.09	14.80
	2-3	0.06	13.40
	3-4	0.07	14.50
	4-5	0.07	15.00
	5-6	0.07	14.80
	6-7	0.07	13.90
	7-8	0.11	13.70
N-ter H4	1-2	0.10	13.20
	2-3	0.10	13.90
	3-4	0.06	13.70
	4-5	0.20	14.40
N-ter H2A	1-2	0.08	13.40
	2-3	0.09	14.50
	3-4	0.03	11.00
C-ter H2A	1-2	0.07	14.10
	2-3	0.07	12.60
N-ter H2B	1-2	0.08	13.50
	2-3	0.10	12.70
	3-4	0.08	15.20
	4-5	0.08	14.20

Linker Histone For linker histones H1E, whose coarse grained model contains 6 beads for the GH and 22 beads for the C-terminal domain (CTD), as shown in Figure 1, the stretching energy is calculated as the summation of the stretching energy between all adjacent beads in the CTD and the single bead in the GH connected to the CTD as follows:

$$E_{lhS} = \sum_{i=1}^{N_{lh}}\sum_{j=1}^{N_i}\frac{k_j}{2}(l_{ij} - l_{j0})^2, \tag{9}$$

where N_{lh} is the number of nucleosome cores that have LH attached and N_i is the number of beads used to calculate the stretching energy. The constant $k_j = 0.1\ kcal/mol/\text{Å}$ and $l_{j0} = 15$ Å for the CTD beads, and $l_{j0} = 0$ for the GH beads connected to the CTD.

3.2 Bending

The bending energy is also based on the Hooke's law, which is given by:

$$E_{B_i} = \frac{g}{2}(\beta_i - \beta_0)^2, \tag{10}$$

where g is the bending constant, β_i the Euler angle described in Section 2.2, and β_0 the equilibrium angle.

The bending energy for linker DNA and nucleosome cores, histone tails, and LHs is calculated as described below.

Linker DNA – Nucleosome Core The bending energy between the linker DNA and nucleosome cores is calculated based on the Euler frames as follows:

$$E_B = \frac{g}{2}\sum_{i=1}^{N-1}\beta_i^2 + \frac{g}{2}\sum_{i\in I_C}(\beta_i^+)^2, \tag{11}$$

where g is the bending rigidity of the DNA with $g = \frac{L_P k_B T}{l_0}$, and $L_P = 50\ nm$ is the persistence length of the DNA. Again, β^+ represents the Euler transformation from $\{\boldsymbol{a}_i^+, \boldsymbol{b}_i^+, \boldsymbol{c}_i^+\}$ to $\{\boldsymbol{a}_i^{DNA}, \boldsymbol{b}_i^{DNA}, \boldsymbol{c}_i^{DNA}\}$ shown in Figure 2.

Histone Tails Similar to the stretching energy calculation, the bending energy for histone tails is the summation of all the bending energies calculated by each tail on all the nucleosome cores.

$$E_{tB} = \sum_{i=1}^{N_c}\sum_{j=1}^{N_t}\sum_{k=1}^{N_j-2}\frac{k_{\beta_{jk}}}{2}(\beta_{ijk} - \beta_{jk0})^2, \tag{12}$$

Parameters $k_{\beta_{jk}}$ and β_{jk0} are taken from our early work in [13], as in Table 2.

Table 2: Histone tails parameters for the bending energy term

Tail	Angle i-j-k	$k_{\beta_{jk}}$ $(kcal/mol/rad^2)$	β_{jk0} $[^o]$
N-ter H3	1-2-3	1.10	115.90
	2-3-4	1.00	116.70
	3-4-5	1.70	117.30
	4-5-6	1.20	123.00
	5-6-7	1.20	111.80
	6-7-8	1.50	114.90
N-ter H4	1-2-3	1.00	112.50
	2-3-4	1.10	116.30
	3-4-5	0.50	111.60
N-ter H2A	1-2-3	1.10	121.20
	2-3-4	0.60	100.10
C-ter H2A	1-2-3	1.00	113.80
N-ter H2B	1-2-3	0.90	118.40
	2-3-4	0.60	118.90
	3-4-5	1.60	124.50

Linker Histone The bending energy is calculated as the summation of the bending energy between all adjacent beads in the CTD and the single bead of the GH connected to the nucleosome:

$$E_{lhB} = \sum_{i=1}^{N_{lh}}\sum_{j=1}^{N_i-1}\frac{k_{\beta_j}}{2}(\beta_{ij} - \beta_{j0})^2, \tag{13}$$

where $k_{\beta_j} = 1$ and $\beta_{j0} = 110^o$. For positions of the 3 adjacent beads on linker histone defined as r_{i-1}, r_i, and r_{i+1}, the angle β_i is defined as:

$$\beta_i = \arccos\left(\frac{(r_i - r_{i-1})\cdot(r_{i+1} - r_i)}{||(r_i - r_{i-1})||||(r_{i+1} - r_i)||}\right). \tag{14}$$

3.3 Twisting

The twisting energy is only applied to linker DNA and nucleosome cores and is given by:

$$E_T = \frac{s}{2l_0} \sum_{i=1}^{N-1} (\alpha_i + \gamma_i - \phi_0)^2, \tag{15}$$

where $s = 3.0 \times 10^{-12}$ $erg\ nm$ is the torsional rigidity constant of DNA as obtained from experiments [15], α and γ are Euler angles, and ϕ_0 is a twist deviation penalty term.

To justify the twisting due to DNA, ϕ_0 is calculated as follows: considering the average rise between B-DNA base pairs 3.4 Å, and average twist 34.95^o; let the number of beads between two nucleosomes be nb, then:

$$\begin{aligned}
number_of_base_pair &= \frac{(nb+1) \times 3}{rise} \\
number_of_turns &= \frac{number_of_base_pairs}{10.3} \\
DNA_rotation &= round(number_of_turns) \\
rotation_per_base_pair &= \frac{DNA_rotation \times 360}{number_of_base_pairs} \\
DNA_twist &= rotation_per_base_pair - twist \\
whole_linker_twist &= number_of_base_pairs \times DNA_twist \\
\phi_0 &= \frac{whole_linker_twist}{nb+1}
\end{aligned} \tag{16}$$

3.4 Electrostatics

The electrostatic energy is calculated using the Debye-Hückel screened electrostatic potential, which is given by:

$$U_{DH}(q_i, q_j, r_{i,j}) = \frac{q_i q_j}{4\pi\varepsilon_0 \varepsilon r_{i,j}} exp(-\kappa r_{i,j}), \tag{17}$$

where q_i, q_j are the charges on the two beads, $r_{i,j}$ the distance between the two beads, ε the dielectric constant, and κ the inverse Debye length.

Electrostatic energies are calculated for all pairs not connected by virtual bonds. For the DNA – nucleosome core interaction, we use a cut off distance of 25 nm, and for all the other type of interactions, we use a cut off distance of 7 nm.

Linker DNA – Nucleosome Core The electrostatic energy between linker DNA and nucleosome cores is calculated using the charge on the linker DNA beads and the 300 charge beads on the nucleosome cores as follows:

$$E_C = \sum_{\substack{j>i+1 \\ i,j \in I_l}}^{N} U_{DH}(q_i, q_j, r_{i,j}) + \sum_{\substack{j>i+1 \\ i \in I_l \\ j \in I_c}}^{N} \sum_{k=1}^{N_c} U_{DH}(q_i, q_{jk}, r_{i,jk}) + \sum_{\substack{j>i \\ i,j \in I_c}}^{N} \sum_{k=1}^{N_c} \sum_{l=1}^{N_c} U_{DH}(q_{ik}, q_{jl}, r_{ik,jl}). \tag{18}$$

Here, N_c is the number of charge beads on the nucleosome cores. The first, second, and third term correspond to the interaction between linker DNA beads, interaction between linker DNA beads and nucleosome cores, and the interaction between nucleosome cores, respectively.

Histone Tails

Histone Tails – Histone Tails The electrostatic energy for tails is calculated between the beads from different tails or the non-adjacent beads from the same tail as follows:

$$E_{tC} = \sum_{\substack{i=1 \\ j>i+2 \\ i,j \in t_a}}^{N_t} U_{DH}(q_i, q_j, r_{i,j}) + \sum_{\substack{i=1 \\ j=1 \\ i,j \in t_a, t_b}}^{N_t} U_{DH}(q_i, q_j, r_{i,j}) \tag{19}$$

Histone Tails – Linker DNA The electrostatic energy is calculated between all histone tail beads and all linker DNA beads as follows:

$$E_{tlC} = \sum_{i \in I_l}^{N} \sum_{j \in I_t}^{N_t} \sum_{k=1}^{N_j} U_{DH}(q_i, q_j, r_{i,j}) \tag{20}$$

Linker Histone

Linker Histone – Linker Histone The electrostatic energy is calculated between the beads from different LHs as follows:

$$E_{lhC} = \sum_{i=1}^{N_{lh}} \sum_{j=1}^{N_i} \sum_{k \neq i}^{N_{lh}} \sum_{l=1}^{N_k} U_{DH}(q_j, q_l, r_{j,k}) \tag{21}$$

Linker Histone – Linker DNA The electrostatic energy is calculated between all LH beads and all linker DNA beads as follows:

$$E_{lhlC} = \sum_{i=1}^{N} \sum_{j=1}^{N_{lh}} \sum_{k=1}^{N_j} U_{DH}(q_i, q_k, r_{i,j}) \tag{22}$$

Linker Histone – Nucleosome Core The electrostatic energy is calculated between all LH beads and the charged beads on non-parental nucleosome cores as follows:

$$E_{lhcC} = \sum_{\substack{i=1 \\ i \in I_{c_a}}}^{N_{lh}} \sum_{j=1}^{N_i} \sum_{\substack{k=1 \\ k \notin I_{c_a}}}^{N_c} U_{DH}(q_j, q_k, r_{i,j}) \tag{23}$$

Linker Histone – Histone Tail The electrostatic energy is calculated between all LH beads and all histone-tail beads as follows:

$$E_{lhtC} = \sum_{i=1}^{N_t} \sum_{j=1}^{N_i} \sum_{k=1}^{N_{lh}} \sum_{l=1}^{N_k} U_{DH}(q_j, q_l, r_{i,j}) \tag{24}$$

3.5 Excluded Volume

The excluded volume energy is calculated using the Lennard-Jones potential given by:

$$U_{LJ}(\sigma, k_{ev}, r_{i,j}) = k_{ev}\Big[\Big(\frac{\sigma}{r_{i,j}}\Big)^{12} - \Big(\frac{\sigma}{r_{i,j}}\Big)^{6}\Big], \tag{25}$$

where k_{ev} is the excluded volume interaction energy parameter, and σ is the effective diameter of the two interacting beads.

We use a cutoff distance of 4 nm to calculate excluded volume energies between linker DNA - linker DNA, linker DNA - nucleosome cores, histone tails - histone tails, histone tails - linker DNA, linker histone - linker histone, linker histone - linker DNA, linker histone - nucleosome cores, and linker histone - histone tails.

Linker DNA – Nucleosome Core There are two types of excluded volume interactions, the interaction between linker DNA and nucleosome cores, and the interaction between different nucleosome cores. The excluded volume is given by:

$$E_V = \sum_{\substack{j>i+1 \\ i \in I_l \\ j \in I_c}}^{N} \sum_{k=1}^{N_c} U_{LJ}(\sigma_{lc}, k_{ev}, r_{i,jk}) + \sum_{\substack{j>i \\ i,j \in I_c}}^{N} \sum_{k=1}^{N_c} \sum_{l=1}^{N_c} U_{LJ}(\sigma_{cc}, k_{ev}, r_{ik,jl}) \tag{26}$$

Here, $k_{ev} = 0.001 k_B T$, $\sigma_{lc} = 2.4\ nm$, and $\sigma_{cc} = 1.2\ nm$.

Histone Tails

Histone Tails – Histone Tails The excluded volume energy for tails is calculated between the beads from different tails or the non-adjacent beads from the same tail as follows:

$$E_{tV} = \sum_{\substack{i=1 \\ j>i+2 \\ i,j\in t_a}}^{N_t} U_{LJ}(\sigma, k_{ev}, r_{i,j}) + \sum_{\substack{i=1 \\ j=1 \\ i,j\in t_a,t_b}}^{N_t} U_{LJ}(\sigma, k_{ev}, r_{i,j}) \tag{27}$$

Histone Tails – Linker DNA The excluded volume energy is calculated between all histone tails beads and all linker DNA beads as follows:

$$E_{tlV} = \sum_{i\in I_l}^{N} \sum_{j\in I_t}^{N_t} \sum_{k=1}^{N_j} U_{LJ}(\sigma, k_{ev}, r_{i,k}) \tag{28}$$

Linker Histone

Linker Histone – Linker Histone The excluded volume energy is calculated between the beads from different LHs and non-adjacent beads on the same LH as follows:

$$E_{lhV} = \sum_{i=1}^{N_{lh}} \sum_{j=1}^{N_i} \sum_{k\neq i}^{N_{lh}} \sum_{l=1}^{N_k} U_{LJ}(\sigma, k_{ev}, r_{j,l}) + \sum_{i=1}^{N_{lh}} \sum_{j=1}^{N_i-2} \sum_{k=i+2}^{N_i} U_{LJ}(\sigma, k_{ev}, r_{j,k}) \tag{29}$$

Linker Histone – Linker DNA The excluded volume energy is calculated between all LH beads and all linker DNA beads as follows:

$$E_{lhlV} = \sum_{i=1}^{N} \sum_{j=1}^{N_{lh}} \sum_{k=1}^{N_j} U_{LJ}(\sigma, k_{ev}, r_{i,k}) \tag{30}$$

Linker Histone – Nucleosome Core The excluded volume energy is calculated between the beads on the LH and the charge beads on the non-attached nucleosome cores as follows:

$$E_{lhcV} = \sum_{\substack{i=1 \\ i\in I_{c_a}}}^{N_{lh}} \sum_{j=1}^{N_i} \sum_{\substack{k=1 \\ k\notin I_{c_a}}}^{N_c} U_{LJ}(\sigma, k_{ev}, r_{i,k}) \tag{31}$$

Linker Histone – Histone Tail The excluded volume energy is calculated between all LH beads and all histone tails beads as follows:

$$E_{lhtV} = \sum_{i=1}^{N_t} \sum_{j=1}^{N_i} \sum_{k=1}^{N_{lh}} \sum_{l=1}^{N_k} U_{LJ}(\sigma, k_{ev}, r_{j,l}) \tag{32}$$

Table 3: Linker histone parameters for the electrostatic and excluded volume energy terms

	charge	$k_{ev_{hh}}$	$k_{ev_{hc}}$	$k_{ev_{hl}}$	$k_{ev_{ht}}$
Global Head					
1	-3.29	1.4360	1.7134	2.2180	1.6180
2	4.22	1.4720	1.7368	2.2360	1.6360
3	8.48	1.4460	1.7199	2.2230	1.6230
4	0.28	1.5380	1.7797	2.2690	1.6690
5	2.08	1.6180	1.8317	2.3090	1.7090
6	3.27	1.5280	1.7732	2.2640	1.6640
C-term					
1	3.36	1.8000	1.8000	2.7000	1.8000
2	0.00	1.8000	1.8000	2.7000	1.8000
3	5.04	1.8000	1.8000	2.7000	1.8000
4	1.68	1.8000	1.8000	2.7000	1.8000
5	3.36	1.8000	1.8000	2.7000	1.8000
6	3.36	1.8000	1.8000	2.7000	1.8000
7	3.36	1.8000	1.8000	2.7000	1.8000
8	1.68	1.8000	1.8000	2.7000	1.8000
9	5.04	1.8000	1.8000	2.7000	1.8000
10	3.36	1.8000	1.8000	2.7000	1.8000
11	3.36	1.8000	1.8000	2.7000	1.8000
12	1.68	1.8000	1.8000	2.7000	1.8000
13	3.36	1.8000	1.8000	2.7000	1.8000
14	5.04	1.8000	1.8000	2.7000	1.8000
15	5.04	1.8000	1.8000	2.7000	1.8000
16	1.68	1.8000	1.8000	2.7000	1.8000
17	3.36	1.8000	1.8000	2.7000	1.8000
18	3.36	1.8000	1.8000	2.7000	1.8000
19	3.36	1.8000	1.8000	2.7000	1.8000
20	3.36	1.8000	1.8000	2.7000	1.8000
21	5.04	1.8000	1.8000	2.7000	1.8000
22	5.04	1.8000	1.8000	2.7000	1.8000

4 Force and Torque

4.1 Force

The force $\mathbf{F}$ on the system is defined as the negative gradient with respect to the position vector collection:

$$\mathbf{F} = -\nabla_r E, \tag{33}$$

where E is the sum of all the interaction energies, and each component of the force $\mathbf{F}_i = -\nabla_{r_i} E$. Following are the details on how each force term is calculated.

Stretching For each bond i, the magnitude of stretching force is calculated by the derivative of Equation 6:

$$F_{S_i} = h(l_i - l_0). \tag{34}$$

Let B_a and B_b be the two DNA beads connected by bond i, and the direction pointing from B_a to B_b be $\vec{r}_{ab}$, then the forces applied to the DNA beads are $F_{B_a} = F_{S_i} \frac{\vec{r}_{ab}}{|\vec{r}_{ab}|}$ and $F_{B_b} = -F_{S_i} \frac{\vec{r}_{ab}}{|\vec{r}_{ab}|}$ (Figure 4).

Bending For each β, the magnitude of bending force is calculated by the derivative of Equation 10:

$$F_{B_i} = g(\beta_i - \beta_0) \tag{35}$$

Similar to the stretching force, after calculating F_{B_i}, we calculate the projection along each pair of DNA beads, and then the force applied on each bead. Instead of two beads involved in stretching, there are three beads involved in bending (Figure 4).

Twisting The twisting force, which describes the change in the torsions $(\alpha_{i-2}+\gamma_{i-2})$, $(\alpha_{i-1}+\gamma_{i-1})$, and $(\alpha_i+\gamma_i)$ created by a change in the position of the i^{th} particle, is defined similarly as we did before [1]:

$$F_T = \frac{s}{l_0}(\chi_i + \xi_i - \chi_{i-1} - \xi_{i-1}), \tag{36}$$

where the vectors χ_i and ξ_i are given by:

$$\chi_i = \frac{(\alpha_i+\gamma_i)}{l_i}\tan\frac{\beta_i}{2}(\cos\alpha_i\vec{c_i} - \sin\alpha_i\vec{b_i}) \tag{37}$$

$$\xi_i = \frac{(\alpha_{i-1}+\gamma_{i-1})}{l_i}\tan\frac{\beta_{i-1}}{2}(\cos\gamma_{i-1}\vec{c_i} + \sin\gamma_{i-1}\vec{b_i}) \tag{38}$$

Electrostatics For each pair of beads i, j, the electrostatic force is calculated by the derivative of Equation 17:

$$F_C = -\frac{q_i q_j(\kappa r_{i,j}+1)}{4\pi\varepsilon_0\varepsilon r_{i,j}^2}exp(-\kappa r_{i,j}) \tag{39}$$

Similar to the stretching force, we calculate the projections and apply the force to the two beads affected (Figure 4).

Exclude Volume For each pair of beads i, j, the exclude volume force is calculated by the derivative of Equation 25:

$$F_V = k_{ev}\Big[\frac{6\sigma^6}{r_{i,j}^7} - \frac{12\sigma^{12}}{r_{i,j}^{13}}\Big] \tag{40}$$

Similar to the stretching force, we calculate the projections and apply the force to the two beads affected (Figure 4).

4.2 Force Projection

As mentioned above, the forces are projected onto two or three beads. Below, we give the details of force projection:

Force projection onto two beads As shown in Figure 4a, the force vector is calculated as:

$$\begin{aligned}\boldsymbol{F}_i &= F\frac{\boldsymbol{r}_{ij}}{|\boldsymbol{r}_{ij}|}\\ \boldsymbol{F}_j &= F\frac{\boldsymbol{r}_{ji}}{|\boldsymbol{r}_{ji}|}\end{aligned} \tag{41}$$

Force projection onto three beads As shown in Figure 4b, the force vector is calculated as:

$$\begin{aligned}\boldsymbol{F}_i &= \frac{F}{|\boldsymbol{r}_{i,i+1}|}\frac{\boldsymbol{r}_{i+1,i}\times(\boldsymbol{r}_{i+1,i}\times\boldsymbol{r}_{i+1,i+2})}{|\boldsymbol{r}_{i+1,i}\times(\boldsymbol{r}_{i+1,i}\times\boldsymbol{r}_{i+1,i+2})|}\\ \boldsymbol{F}_{i+2} &= \frac{F}{|\boldsymbol{r}_{i+1,i+2}|}\frac{\boldsymbol{r}_{i+2,i+1}\times(\boldsymbol{r}_{i+1,i}\times\boldsymbol{r}_{i+1,i+2})}{|\boldsymbol{r}_{i+2,i+1}\times(\boldsymbol{r}_{i+1,i}\times\boldsymbol{r}_{i+1,i+2})|}\\ \boldsymbol{F}_{i+1} &= -\boldsymbol{F}_i - \boldsymbol{F}_{i+2}\end{aligned} \tag{42}$$

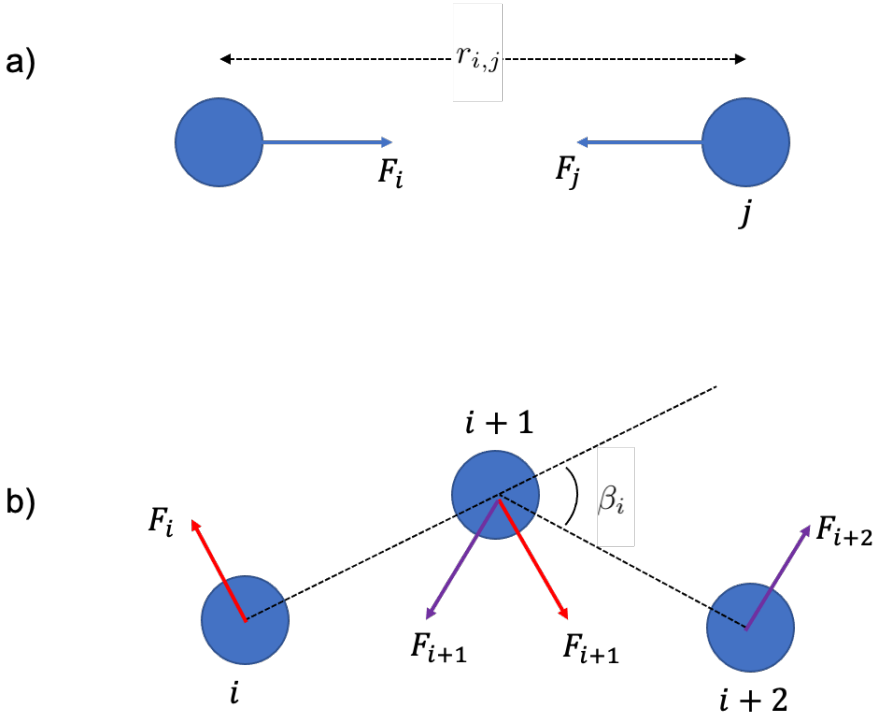

Figure 4: Force projection after calculating the magnitude of the forces. a). Force projection onto two beads, which is used in the case of stretching, electrostatics, and excluded volume forces. b) Force projection onto three beads, which is used in the case of bending force.

4.3 Torque

There are two types of torques applied during the simulation: torques due to the forces and mechanical torques due to the twisting potential in Equation 15.

Torque due to force The torques due to the forces are calculated by the equation:

$$\tau = \mathbf{r} \times \mathbf{F}, \tag{43}$$

where $\boldsymbol{r}$ is the positional vector away from the center, and $\boldsymbol{F}$ is the force vector calculated above. Note that linker DNA, histone tails, and linker histones are represented only by beads so that there is no torque due to forces applied on them. For nucleosome cores, the torques are generated by the two imaginary points when calculating stretching, bending, and twisting forces, and by the 300 charge beads when calculating electrostatics and excluded volume forces.

Mechanical torque The mechanical torques for linker DNA are due to the twisting potential and are only applied in the longitudinal direction $\boldsymbol{a}$, given by:

$$\tau_i = -\frac{s}{l_0}(\alpha_i + \gamma_i - \alpha_{i-1} - \gamma_{i-1}), \tag{44}$$

Besides the torque acting in direction $\boldsymbol{a}$, there are also torques in directions $\boldsymbol{b}$ and $\boldsymbol{c}$ acting on nucleosome cores. Thus, the total torque for nucleosome cores can be written as:

$$\tau_i = \tau_i^F + \tau_i^B + \tau_i^T, \tag{45}$$

where τ_i^F is the torque due to forces, τ_i^B the torque due to bending potential, and τ_i^T the torque due to twisting potential.

4.4 Testing

We have tested the correctness of the derivatives by checking the ratio of the Taylor expansion described below:

A Taylor series expansion for a multivariate function E at $\mathbf{x}_k + \mathbf{p}$, where $\mathbf{p}$ is the displacement vector:

$$E(\mathbf{x}_k + \mathbf{p}) \approx E(\mathbf{x}_k) + \mathbf{g}_k^T \mathbf{p} + \frac{1}{2}\mathbf{p}^T H_k \mathbf{p}. \tag{46}$$

where $\mathbf{x}_k$ is the current approximation to the solution vector $\mathbf{x}^*$, and $\mathbf{g}_k$ and H_k are the gradient and Hessian evaluated at $\mathbf{x}_k$ respectively.

For $\mathbf{p} = \varepsilon\mathbf{Y}$, with $\mathbf{Y}$ is a random perturbation vector and ε is a scalar, we have:

$$E(\mathbf{x}_k + \varepsilon\mathbf{Y}) = E(\mathbf{x}_k) + \varepsilon\mathbf{g}_k^T\mathbf{Y} + \frac{\varepsilon^2}{2}\mathbf{Y}^T H_k \mathbf{Y} + O(\varepsilon^3). \tag{47}$$

If only the gradient is tested, we have:

$$E(\mathbf{x}_k + \varepsilon\mathbf{Y}) = E(\mathbf{x}_k) + \varepsilon\mathbf{g}_k^T\mathbf{Y} + O(\varepsilon^2). \tag{48}$$

When we divide ε by 2, we have:

$$E\Big(\mathbf{x}_k + \frac{\varepsilon}{2}\mathbf{Y}\Big) = E(\mathbf{x}_k) + \frac{\varepsilon}{2}\mathbf{g}_k^T\mathbf{Y} + O\Big(\Big(\frac{\varepsilon}{2}\Big)^2\Big). \tag{49}$$

Then, the ratio tested is $O(\varepsilon^2)/O((\frac{\varepsilon}{2})^2) = 4$.

We divide ε by 2 at every step and test if indeed our truncation errors decrease with the expected rate (i.e., for a correct gradient, if the error corresponding to ε is $E1$, then the error for $\varepsilon/2$ should be $E1/4$).

The following table shows that with decreasing ε, the ratio becomes closer to 4, supporting that the analytical solutions for the forces are correct.

Table 4: Ratio with decreasing ε

Ratio	ε
21499.5	0.5
4.20064	0.25
4.10839	0.125
4.05615	0.0625
4.02855	0.03125
4.0144	0.015625
4.00723	0.0078125
4.00362	0.00390625
4.00181	0.00195312
4.00091	0.000976562
4.00045	0.000488281
4.00023	0.000244141
4.0001	0.00012207
4.00002	6.10352×10^{-5}
4.00001	3.05176×10^{-5}

5 Hydrodynamic Interactions

5.1 Translational hydrodynamics

In Brownian dynamics, the movements of the particles of the chromatin system are coupled to one another through the action of the viscous medium. The hydrodynamic friction tensor, $\mathbf{H}$, is then introduced to approximate this viscous coupling. The diffusion tensor $\mathbf{D}$ is proportional to $\mathbf{H}$ in Brownian dynamics algorithm with $\mathbf{D} = k_B T\mathbf{H}$.

For an N-bead system, $\mathbf{D}$ is a $3N \times 3N$ matrix:

$$\mathbf{D} = \begin{bmatrix} \mathbf{D}_{11} & \mathbf{D}_{12} & \dots & \mathbf{D}_{1N} \\ \mathbf{D}_{21} & \mathbf{D}_{22} & \dots & \mathbf{D}_{2N} \\ \vdots & \vdots & & \vdots \\ \mathbf{D}_{N1} & \mathbf{D}_{N2} & \dots & \mathbf{D}_{NN} \end{bmatrix}, \tag{50}$$

where each $\mathbf{D}_{ij}$ is a 3×3 matrix for the interaction between bead$_i$ and bead$_j$.

There are two types of diffusion tensors introduced in [11], the Oseen and Rotne-Prager tensors. Our approach uses the Rotne-Prager tensor because in the BD simulation the diffusion tensor needs to be a positive definite matrix to apply the Cholesky decomposition. The Oseen tensor becomes non-positive definite when the separation between the particles is small. The Rotne-Prager tensor is given by:

$$\mathbf{D}_{ij} = \left\{ \begin{array}{ll} \frac{k_B T}{6\pi\eta a_i}\mathbf{I}, & \text{for } i = j \\ \frac{k_B T}{8\pi\eta r_{i,j}} \left[\left(\mathbf{I} + \frac{\mathbf{r}_{i,j}\mathbf{r}_{i,j}}{r_{i,j}^2} \right) + \frac{(a_i^2 + a_j^2)}{r_{i,j}^2} \left(\frac{1}{3}\mathbf{I} - \frac{\mathbf{r}_{i,j}\mathbf{r}_{i,j}}{r_{i,j}^2} \right) \right], & \text{for } i \neq j \end{array} \right\}, \tag{51}$$

where η is the solvent viscosity and a is the sphere radius of the particles.

The above formula is for the two non-overlapping particles, i, j. For overlapping particles, we use:

$$\mathbf{D}_{ij} = \frac{k_B T}{6\pi\eta a_{eff}} \left[\left(1 - \frac{9}{32}\frac{r_{i,j}}{a_{eff}} \right)\mathbf{I} + \frac{3}{32}\frac{\mathbf{r}_{i,j}\mathbf{r}_{i,j}}{a_{eff} r_{i,j}} \right]. \tag{52}$$

Here $a_{eff} = \sqrt{a_i^2 + a_j^2}$, which has been proven for $a_i = a_j$ [16], and has been proposed for $a_i \neq a_j$ [13, 17].

All the particles (including nucleosome cores) are treated as spheres for hydrodynamic interactions purposes. The choice of radius for linker DNA, nucleosome cores, histone tails and LHs are 1.5 nm, 5.0 nm, 0.6 nm, and 0.5 nm, respectively. The radius of the core (a_{core}) is based on the diffusion coefficient D measured in [18], and use the relation of $D = k_B T / 6\pi\eta a_{core}$. This radius choice of the core bead is nearly equal to the volume of a disk of radius 6 nm and width 5nm. The radius for other beads (DNA, tails, LHs) are based on our touching-bead model, and the values are calculated by $a_x = \dfrac{length\ of\ string_x}{2 \times number\ of\ beads}$, ($x$ = DNA, tail, LH).

5.2 Rotational hydrodynamics

Since we only calculate torque for the linker DNA and nucleosome cores, the rotational friction is only applied to these beads. The rotational frictional coefficients adopted from [1] can be expressed as:

$$\xi_{a_i} = \xi_{b_i} = \xi_{c_i} = 8\pi\eta a_{core}^3 \tag{53}$$

for nucleosome cores, and

$$\xi_{a_i} = 8\pi\eta a_{DNA}^3 \tag{54}$$

for linker DNA, since DNA beads only rotate about the $\mathbf{a}_i$ axis.

6 Brownian Dynamics Algorithm

A commonly used Brownian Dynamics algorithm was first proposed in 1978 [11] based on the Langevin equation, then improved in 1989 [19] with second-order algorithm based on the Runge-Kutta method to overcome the issue of inefficient procedure and unstable numerical behaviour introduced by the first-order approximation when the time step is small. In 2001, Beard and Schlick [1] further modified the second-order BD algorithm and this is adopted in this paper.

6.1 First-order estimate

6.1.1 translation

The first-order translational update (at nth step) is given by:

$$\mathbf{r}^{n+1,*} = \mathbf{r}^n + \frac{\Delta t}{k_B T}\mathbf{D}(\mathbf{r}^n)\mathbf{F}^n + \mathbf{R}^n \tag{55}$$

where $\mathbf{r}$ is the position vector, Δt is the time step, k_B is the Boltzmann's constant, T is the absolute temperature, $\mathbf{D}$ is the diffusion tensor, $\mathbf{F}$ is the force, and $\mathbf{R}$ is the stochastic random force, which is a Gaussian distributed random vector with zero mean and covariance of:

$$\left\langle \mathbf{R}^n(\Delta t)(\mathbf{R}^m(\Delta t))^T \right\rangle = 2\mathbf{D}^n \Delta t \delta_{nm} \tag{56}$$

6.1.2 rotation

The first-order rotational update (at nth step) is given by:

$$\begin{aligned} \Delta\Omega_{a_i}^{n,*} &= \frac{\Delta t}{\xi_{a_i}}(\tau_{a_i}^n + \omega_{a_i}^n) \\ \Delta\Omega_{b_i}^{n,*} &= \frac{\Delta t}{\xi_{b_i}}(\tau_{b_i}^n + \omega_{b_i}^n) \\ \Delta\Omega_{c_i}^{n,*} &= \frac{\Delta t}{\xi_{c_i}}(\tau_{c_i}^n + \omega_{c_i}^n) \end{aligned} \tag{57}$$

where $\{\Delta\Omega_{a_i}^{n,*}, \Delta\Omega_{b_i}^{n,*}, \Delta\Omega_{c_i}^{n,*}\}$ is the finite rotation of the ith particle about its local coordinate system $\{\mathbf{a}_i^n, \mathbf{b}_i^n, \mathbf{c}_i^n\}$, τ is the torque, ξ_{a_i,b_i,c_i} is the rotational friction coefficient, and ω_i is the stochastic terms, with zero mean Gaussian distributions and variance of:

$$\begin{aligned} \left\langle \omega_{a_i}^n(\Delta t)\omega_{a_i}^m(\Delta t) \right\rangle &= 2k_BT\xi_{a_i}\delta_{nm} \\ \left\langle \omega_{b_i}^n(\Delta t)\omega_{b_i}^m(\Delta t) \right\rangle &= 2k_BT\xi_{b_i}\delta_{nm} \\ \left\langle \omega_{c_i}^n(\Delta t)\omega_{c_i}^m(\Delta t) \right\rangle &= 2k_BT\xi_{c_i}\delta_{nm} \end{aligned} \tag{58}$$

where δ_{nm} is the Kroneker delta.

By applying the rotation matrix $\Delta\Omega_i^{n,*}$ calculated above to the Euler frames $\{\boldsymbol{a}_i^n, \boldsymbol{b}_i^n, \boldsymbol{c}_i^n\}$ at nth step, we can obtain the first-order estimate of the Euler frames $\{\boldsymbol{a}_i^{n+1,*}, \boldsymbol{b}_i^{n+1,*}, \boldsymbol{c}_i^{n+1,*}\}$. With the rotation only applying to nucleosome cores and the $\mathbf{a}_i$ axes of the linker DNAs.

6.2 Second-order estimate

With first-order estimate of the translation and rotation at time $(n+1)\Delta t$ ($\Delta\mathbf{r}^{n,*}$ and $\Delta\Omega_i^{n,*}$), we calculate the forces $\mathbf{F}^{n+1,*}$ and torques $\tau_i^{n+1,*}$ at the end of $n+1$ time step based on $\mathbf{r}^{n+1,*}$ and $\{\boldsymbol{a}_i^{n+1,*}, \boldsymbol{b}_i^{n+1,*}, \boldsymbol{c}_i^{n+1,*}\}$, then use them to construct an explicit second-order update.

6.2.1 translation

The second-order translational update (at nth step) is given by:

$$\mathbf{r}^{n+1} = \mathbf{r}^n + \frac{\Delta t}{2k_BT}\mathbf{D}(\mathbf{r}^n)(\mathbf{F}^n + \mathbf{F}^{n+1,*}) + \mathbf{R}^n \tag{59}$$

6.2.2 rotation

The second-order rotational update (at nth step) is given by:

$$\begin{aligned} \Delta\Omega_{a_i}^n &= \frac{\Delta t}{\xi_{a_i}}((\tau_{a_i}^n + \tau_{a_i}^{n+1,*})/2 + \omega_{a_i}^n) \\ \Delta\Omega_{b_i}^n &= \frac{\Delta t}{\xi_{b_i}}((\tau_{b_i}^n + \tau_{b_i}^{n+1,*})/2 + \omega_{b_i}^n) \\ \Delta\Omega_{c_i}^n &= \frac{\Delta t}{\xi_{c_i}}((\tau_{c_i}^n + \tau_{c_i}^{n+1,*})/2 + \omega_{c_i}^n) \end{aligned} \tag{60}$$

6.3 Cholesky decomposition

The Cholesky approach is used to compute $\mathbf{R}$ to satisfy the proprieties of Eq. (56). The Cholesky decomposition of the diffusion tensor $\mathbf{D}$ is determined by $\mathbf{D} = \mathbf{L}\mathbf{L}^T$, where $\mathbf{L}$ is a lower triangular matrix and each element in $\mathbf{L}$ is given by:

$$l_{ij} = \left\{ \begin{array}{ll} (D_{ii} - \sum_{k=1}^{i-1} l_{ik}^2)^{\frac{1}{2}}, & \text{if } i = j \\ (D_{ij} - \sum_{k=1}^{j-1} l_{ik}l_{jk})/s_{jj}, & \text{if } i > j \\ 0, & \text{if } i < j \end{array} \right\}, \tag{61}$$

7 Summary of parameters used in the simulations

We adopt parameters mainly from previous works in Schlick's lab [1, 13] and unified the units. Below is a summary of the parameters used in our program.

Table 5: Parameters used in the BD simulation

Parameter	Description	Value
T	Temperature	293.15 K
Δt	time step	10^{-12} s
k_B	Boltzmann constant	1.380649×10^{-5} $(nm^2 \cdot kg)/(s^2 \cdot K)$
η	viscosity of the surrounding fluid	1.137076×10^{-12} $kg/(nm \cdot s)$
a_{core}	hydrodynamic radius of the core	5.0 nm
a_{DNA}	hydrodynamic radius of DNA	1.2 nm
ξ_{core}	rotational frictional coefficient of the core	$8\pi\eta d_{core}^3$
ξ_{DNA}	rotational frictional coefficient of DNA	$8\pi\eta a_{DNA}^3$
l_0	Equilibrium segment length	3.0 nm
r_0	Radius of wound DNA supercoil	4.8 nm
$2\omega_0$	Width of wound DNA supercoil	3.6 nm
h	DNA Stretching constant	$100k_BT/l_0^2$
g	DNA Bending constant	$50k_BT/l_0$ (without Mg) or $30k_BT/l_0$ (with Mg)
C	DNA Twisting constant	$72.429k_BT/l_0$
k_e	Electrostatics parameter	$0.4151k_BT$
k_{ex}	Excluded volume parameter	$0.001k_BT$
$\sigma_{DNA-DNA}$	DNA-DNA excluded volume distance	3.6 nm
$\sigma_{DNA-Core}$	DNA-Core excluded volume distance	2.4 nm
$\sigma_{Core-Core}$	Core-Core excluded volume distance	1.2 nm
$\sigma_{Tail-Tail}$	Tail-Tail excluded volume distance	1.8 nm
$\sigma_{Tail-DNA}$	Tail-DNA excluded volume distance	2.7 nm
$\sigma_{Tail-Core}$	Tail-Core excluded volume distance	1.8 nm

References

[1] D. A. Beard and T. Schlick, "Computational Modeling Predicts the Structure and Dynamics of Chromatin Fiber," *Structure*, vol. 9, no. 2, pp. 105–114, 2001.

[2] S. Portillo-Ledesma and T. Schlick, "Bridging chromatin structure and function over a range of experimental spatial and temporal scales by molecular modeling," *WIREs Comput. Mol. Sci.*, vol. 10, no. 2, 2020.

[3] G. D. Bascom and T. Schlick, "Chromatin Fiber Folding Directed by Cooperative Histone Tail Acetylation and Linker Histone Binding," *Biophys. J.*, vol. 114, no. 10, pp. 2376–2385, 2018.

[4] Q. Zhang, D. A. Beard, and T. Schlick, "Constructing Irregular Surfaces to Enclose Macromolecular Complexes for Mesoscale Modeling Using the Discrete Surface Charge Optimization (DiSCO) Algorithm," *J. Comput. Chem.*, vol. 24, no. 16, pp. 2063–2074, 2003.

[5] R. Collepardo-Guevara and T. Schlick, "Chromatin fiber polymorphism triggered by variations of DNA linker lengths," *Proc. Natl. Acad. Sci. U. S. A.*, vol. 111, no. 22, pp. 8061–8066, 2014.

[6] G. Arya and T. Schlick, "A tale of tails: how histone tails mediate chromatin compaction in different salt and linker histone environments," *J. Phys. Chem. A*, vol. 113, no. 16, pp. 4045–4059, 2009.

[7] A. Luque, R. Collepardo-Guevara, S. Grigoryev, and T. Schlick, "Dynamic condensation of linker histone C-terminal domain regulates chromatin structure," *Nucleic Acids Res.*, vol. 42, no. 12, pp. 7553–7560, 2014.

[8] R. Collepardo-Guevara, G. Portella, M. Vendruscolo, D. Frenkel, T. Schlick, and M. Orozco, "Chromatin Unfolding by Epigenetic Modifications Explained by Dramatic Impairment of Internucleosome Interactions: A Multiscale Computational Study," *J. Am. Chem. Soc.*, vol. 137, no. 32, pp. 10205–10215, 2015.

[9] G. D. Bascom and T. Schlick, "Chromatin Fiber Folding Directed by Cooperative Histone Tail Acetylation and Linker Histone Binding," *Biophys. J.*, vol. 114, no. 10, pp. 2376–2385, 2018.

[10] O. Perisic, S. Portillo-Ledesma, and T. Schlick, "Sensitive effect of linker histone binding mode and subtype on chromatin condensation," *Nucleic Acids Res.*, vol. 47, no. 10, pp. 4948–4957, 2019.

[11] D. L. Ermak and J. A. McCammon, "Brownian dynamics with hydrodynamic interactions," *J. Chem. Phys.*, vol. 69, no. 4, pp. 1352–1360, 1978.

[12] H. Jian, A. V. Vologodskii, and T. Schlick, "A combined wormlike-chain and bead model for dynamic simulations of long linear DNA," *J. Comput. Phys.*, vol. 136, no. 1, pp. 168–179, 1997.

[13] G. Arya, Q. Zhang, and T. Schlick, "Flexible histone tails in a new mesoscopic oligonucleosome model," *Biophys. J.*, vol. 91, no. 1, pp. 133–150, 2006.

[14] D. A. Beard and T. Schlick, "Modeling salt-mediated electrostatics of macromolecules: The discrete surface charge optimization algorithm and its application to the nucleosome," *Biopolymers*, vol. 58, no. 1, pp. 106–115, 2001.

[15] D. S. Horowitz and J. C. Wang, "Torsional rigidity of DNA and length dependence of the free energy of DNA supercoiling," *J. Mol. Biol.*, vol. 173, no. 1, pp. 75–91, 1984.

[16] J. Rotne and S. Prager, "Variational Treatment of Hydrodynamic Interaction in Polymers," *J. Chem. Phys.*, vol. 50, no. 11, pp. 4831–4837, 1969.

[17] B. Carrasco, J. García de la Torre, and P. Zipper, "Calculation of hydrodynamic properties of macromolecular bead models with overlapping spheres," *Eur. Biophys. J.*, vol. 28, no. 6, pp. 510–515, 1999.

[18] J. Yao, P. T. Lowary, and J. Widom, "Direct detection of linker DNA bending in defined-length oligomers of chromatin," *Proc. Natl. Acad. Sci. U. S. A.*, vol. 87, no. 19, pp. 7603–7607, 1990.

[19] A. Iniesta and J. García De La Torre, "A second-order algorithm for the simulation of the Brownian dynamics of macromolecular models," *J. Chem. Phys.*, vol. 92, no. 3, pp. 2015–2018, 1990.